

Analytical Methods

Accepted Manuscript



This is an *Accepted Manuscript*, which has been through the Royal Society of Chemistry peer review process and has been accepted for publication.

Accepted Manuscripts are published online shortly after acceptance, before technical editing, formatting and proof reading. Using this free service, authors can make their results available to the community, in citable form, before we publish the edited article. We will replace this *Accepted Manuscript* with the edited and formatted *Advance Article* as soon as it is available.

You can find more information about *Accepted Manuscripts* in the [Information for Authors](#).

Please note that technical editing may introduce minor changes to the text and/or graphics, which may alter content. The journal's standard [Terms & Conditions](#) and the [Ethical guidelines](#) still apply. In no event shall the Royal Society of Chemistry be held responsible for any errors or omissions in this *Accepted Manuscript* or any consequences arising from the use of any information it contains.

1
2
3
4
5
6
7
8
9
10
11
12
13
14
15
16
17
18
19
20
21
22
23
24
25
26
27
28
29
30
31
32
33
34
35
36
37
38
39
40
41
42
43
44
45
46
47
48
49
50
51
52
53
54
55
56
57
58
59
60

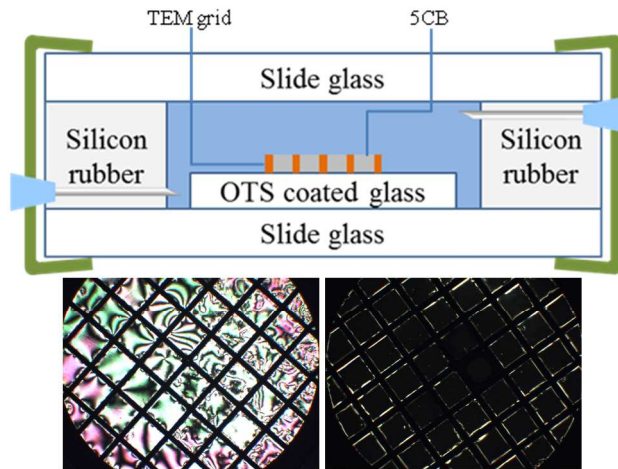


Figure. Graphical abstract

1
2
3
4
5
6
7
8
9
10
11
12
13
14
15
16
17
18
19
20
21
22
23
24
25
26
27
28
29
30
31
32
33
34
35
36
37
38
39
40
41
42
43
44
45
46
47
48
49
50
51
52
53
54
55
56
57
58
59
60

Real-time liquid crystal-based biosensor for urea detection

Mashooq Khan,¹ Young Kyoo Kim,¹ Joon Hyung Lee,² Inn-Kyu Kang¹ and Soo-Young Park^{1}*

¹ School of Applied Chemical Engineering, Kyungpook National University, Daegu 702-701, Republic of Korea

² School of Advanced Materials Engineering, Kyungpook National University, Daegu 702-701, Republic of Korea

* Corresponding author E-mail: psy@knu.ac.kr

1
2
3
4
5
6
7
8
9
10
11
12
13
14
15
16
17
18
19
20
21
22
23
24
25
26
27
28
29
30
31
32
33
34
35
36
37
38
39
40
41
42
43
44
45
46
47
48
49
50
51
52
53
54
55
56
57
58
59
60

KEYWORDS: Biosensor, urease, liquid-crystal, urea, block copolymer, 5CB

Abstract: A transmission electron microscopy (TEM) grid filled with 4-cyano-4'-pentylbiphenyl (5CB) on an octadecyltrichloro silane-coated glass substrate in aqueous media was developed to construct a urea biosensor by coating poly(acrylicacid-b-4-cyanobiphenyl-4-oxyundecylacrylate) (PAA-b-LCP) at the aqueous/5CB interface and immobilizing urease covalently to the PAA chains. Urea was detected from the planar to homeotropic (P-H) orientational transition of 5CB by polarized optical microscopy under crossed polarizers. This TEM grid sensor with the maximum immobilization density of urease, 0.17 molecules/nm², enabled the detection of urea at concentrations as low as 5 mM through a P-H change with the half time of a full P-H change of 250 seconds. This TEM grid sensor could detect urea in the blood without any inference from hemoglobin and ascorbic acid. This new and sensitive urea biosensor is relatively inexpensive, allows easy naked eye detection, and might be useful for screening the urea level in the human body.

1
2
3
4 **Introduction:** The decomposition of the nucleic acids and proteins produces urea as a
5 nitrogenous waste in the liver. Humans have a normal urea level of 0.25-0.6 mM in blood and
6
7 155-390 mM in urine.¹ An increase in the body urea level causes several complications, such as
8
9 renal failure, acute or chronic urinary tract obstruction with shock, burns, dehydration, and
10
11 gastro-intestinal bleeding. On the other hand, a decrease in the blood urea concentration also
12
13 leads to hepatic failure, nephritic syndrome and cachexia.² Measurements of the blood urea are
14
15 the best way of evaluating the body functions and identifying the related diseases. Therefore,
16
17 detection of the body urea level has considerable significance in clinical chemistry and
18
19 biomedical analysis.
20
21
22
23
24

25
26
27 The use of the enzymatic hydrolysis of urea by urease in the development of a urea
28
29 biosensor has attracted considerable attention from biochemical and clinical analysis. The urease
30
31 hydrolysis of urea generates ionic products, such as NH_4^+ , HCO_3^- and OH^- , as shown in scheme
32
33
34 1. Many urea biosensors can measure the concentrations of the ions produced during the
35
36 enzymatic reaction on urease-immobilized membranes, polymers, sol-gels, conducting polymers,
37
38 Langmuir Blodgett films, nanomaterials, self-assembled monolayers, and metal nanoparticles
39
40 and nanocluster-based composites. The ions produced are monitored using several kinds of
41
42 transducers, such as spectrometry, potentiometer with the application of a pH-sensitive electrode,
43
44 an ammonium ion selective field effect transistor, conductometry, coulometry, and
45
46 amperometry.^{1, 3-15} Among these transducers, potentiometric and amperometric methods are used
47
48 frequently. On the other hand, a potentiometric transducer suffers from the sluggish response to
49
50 the solution with low analyte concentrations and vulnerability to the interference of other ions in
51
52 the sample solution. An amperometric transducer normally uses glutamate dehydrogenase in
53
54 addition to urease and shows a high level of interference caused by the oxidation or reduction of
55
56
57
58
59
60

1
2
3
4 commonly encountered compounds in clinical samples, such as acetaminophen and ascorbic acid,
5
6
7 at the working potential, even though it has better sensitivity and a lower detection limit
8
9
10 compared to those obtained using potentiometric methods.

11 The urease hydrolysis of urea produces OH^- ions, which increases the local pH.
12
13 Therefore, monitoring the pH can be used in urea analysis. pH-sensitive glass electrodes are
14
15 available for monitoring the pH in aqueous solutions but they are unsuitable for measuring the
16
17 pH in solutions with small volumes. The aim of this study was to exploit the optical properties of
18
19 liquid crystals (LCs) and design a label-free urea sensor with good spatial resolution for
20
21 monitoring the changes in the localized pH, resulting from the urease activities. LCs have a low
22
23 surface anchoring energy (10^{-3} to 10^{-6} J/m²) at the LC/aqueous interface making them sensitive to
24
25 environmental changes through an ordering transition, which can be propagated within the LC
26
27 mesogens to a distance of ~ 100 μm (10^5 of molecular length).¹⁶ The utility of the LCs to
28
29 transduce and amplify the molecular events at the LC/aqueous interface in response to the
30
31 presence of proteins,^{17, 18} lipids,¹⁹ surfactants,²⁰ synthetic polymers²¹⁻²⁴ and endotoxin²⁵ have
32
33 been reported. Moreover, when these surfactants or polymers contain pH-sensitive functional
34
35 groups, the orientation of the LCs becomes sensitive to the pH in the aqueous phase. For
36
37 example the aqueous/LC interface in transmission electron microscopy (TEM) grids was
38
39 functionalized by poly(ethylene imine) conjugated to N-[3-(dimethyl amino)-propyl]acrylamide)
40
41 to obtain a pH-responsive LC sensor. The pH-dependent change in the orientation of the LCs
42
43 causing its optical appearance was attributed to changes in the chain conformation at the
44
45 LC/water interface.²⁶ Bi et al. developed a TEM-grid pH sensor by doping with 4-
46
47 pentylbiphenyl-4-carboxylic acid (PBA) to visualize the local pH changes from the enzymatic
48
49 hydrolysis of penicillin G by surface-immobilized penicillinase.²⁷ A recent report showed that a
50
51
52
53
54
55
56
57
58
59
60

1
2
3
4
5
6
7
8
9
10
11
12
13
14
15
16
17
18
19
20
21
22
23
24
25
26
27
28
29
30
31
32
33
34
35
36
37
38
39
40
41
42
43
44
45
46
47
48
49
50
51
52
53
54
55
56
57
58
59
60

TEM grid cell functionalized with a pH-responsive amphiphilic poly(acrylic acid-*b*-4-cyanobiphenyl-4-oxyundecylacrylate) (PAA-*b*-LCP) on 5CB exhibited a rapid and reversible homeotropic to planar (H-P) change in 5CB in response to the shrinkage and swelling of PAA chains caused by changes in the pH of the solution.^{21, 22}

In this study, a urea sensor was designed by immobilizing urease on the PAA chains in a TEM grid cell coated with PAA-*b*-LCP at the 5CB/aqueous interface. In response to the pH change brought by the urease-induced hydrolysis reaction of urea, the P-H transition of 5CB occurred through a change in the PAA chain conformation. This LC-based TEM grid urea sensor was tested for the simple detection of small amounts of OH⁻ ions produced from a urease reaction with urea through the naked eye using a polarized optical microscope with crossed polarizers.

Experimental:

Materials: Copper TEM specimen grids (G75 with a grid square width of 285 μm, pitch of 340 μm, bar width of 55 μm, size of 3.05 mm, and thickness of 18 μm) were purchased from Ted Pella, Inc. and cleaned by washing sequentially with acetic acid, acetone and ethanol. The microscope glass slides (Duran group, Germany) and urease type III (E.C. 3.5.1.5) from the jack bean with molecular weight of 4.8×10⁵ g/mole were obtained from Sigma-Aldrich. Urea (Sigma-Aldrich), N-(3-dimethylaminopropyl)-N-ethylcarbodiimide hydrochloride (EDC.HCl, Sigma Aldrich), N-hydroxysulfosuccinimide sodium salt (NHS, Sigma Aldrich), ascorbic acid (Sigma), uric acid (sigma), trifluoroacetic acid (TFA, Aldrich, 99%), 4-cyano-4-pentylbiphenyl (5CB) (TCI, 100%), octadecyl trichloro silane (OTS), N-N,dimethylformamide (DMF) (Sigma-Aldrich), methanol (Aldrich) and dichloromethane (DCM, Aldrich) were used as received. The PAA-*b*-

1
2
3
4 LCP was synthesized using the same method reported in a previous study.²¹ The molecular
5 weight was PAA (11K)-b-LCP (5K) with a PDI of 1.14. Figure supplementary information (SI) 1
6
7 presents its NMR spectrum with the assignments of the protons.
8
9

10
11 **Monolayer formation of PAA-b-LCP:** Monolayer experiments were performed using a
12 Langmuir–Blodgett (LB) KSV Layer builder (KSV Instruments Ltd., AAA100178, Finland)
13 connected to a KSV minimicro trough, which was surrounded by an environmental chamber.
14 The working area of the trough was $17 \times 5 \text{ cm}^2$. All experiments were carried out at room
15 temperature. The surface pressure of the monolayer at the air/liquid interface was measured
16 using a Wilhelmy plate attached to a microbalance. PAA-b-LCP was dissolved in dioxane and
17 kept at 60°C for two days. Subsequently, toluene was added to the dioxane solution to obtain a
18 final concentration of 1 mg/ml with a dioxane to toluene ratio of 6/4 (v/v). When a zero surface
19 pressure was reached, 100 μL of the PAA-b-LCP solution was spread immediately on the water
20 to form a monolayer. One hour after monolayer formation, the monolayer was then compressed,
21 expanded and compressed at a rate of 3 mm/min to achieve equilibrium. The aerial density of the
22 monolayer was controlled by the surface pressure on the spread LB film at 35mN/m (see Figure
23 SI 2).
24
25
26
27
28
29
30
31
32
33
34
35
36
37
38
39
40
41
42

43 **Sensor cell preparation:** A TEM grid flow cell was fabricated using the method reported in the
44 literature.^{18, 21} Briefly, glass microscope slides were cleaned using a piranha solution (**Caution:**
45 piranha solution is extremely corrosive and must be handled carefully), washed subsequently
46 with distilled water, dried under nitrogen and coated with OTS. A copper TEM grid was placed
47 on the surface of $12 \times 8 \text{ mm}^2$ OTS-coated glass substrates that were glued to another common
48 slide glass substrate with epoxy. A 1 μL drop of 5CB was placed on a TEM grid using a 5 μL
49 syringe. The excess 5CB was removed using a capillary tube to obtain a uniform thin film. To
50
51
52
53
54
55
56
57
58
59
60

1
2
3
4 transfer the PAA-b-LCP monolayer to the surface of 5CB in the TEM grid, the TEM grid filled
5
6 with 5CB was inserted slowly into the PAA-b-LCP-spread trough with the TEM grid side
7
8 downward coming to rest on a silicon spacer (2 mm thick) attached to another slide glass in a LB
9
10 bath. Two slide glasses spaced with silicon rubber were then clipped with binder-clips. The inlet
11
12 and outlet ports for exchanging the solutions were made with needles that were punched through
13
14 silicon rubber. The internal volume of the flow cell was 0.4 mL. The flow cell was then flipped
15
16 over and used for further analysis. Figure SI 3 presents a schematic diagram and photograph of
17
18 the flow cell containing a TEM grid cell.
19
20
21
22
23

24 **Immobilization of urease to PAA:** Urease was immobilized on the PAA chains on a TEM grid
25
26 using a slight modification of the method reported elsewhere.²⁸ Briefly, the PAA chains were
27
28 activated with 0.4 M EDC.HCl and 0.1 M NHS for one hour. Subsequently, 6 mL of a urease
29
30 solution was then passed through the flow cell and kept for 12 hours at room temperature, as
31
32 summarized in Scheme 2.
33
34
35

36 The test concentrations of the urease solution (C_{urease}) in the flow cell were 2, 4, 6, 11, 21,
37
38 42 and 63 μM . The concentrations of immobilized urease were determined using a UV-visible
39
40 spectrophotometer (Shimadzu 2401, Japan) with the reference sample of deionized water. The
41
42 calibration curve for urease (Figure SI 4) was obtained in the range, 0 to 20 μM , at a maximum
43
44 absorbance wavelength (λ_{max}) of 276 nm. The amounts of immobilized urease (C_{imb}) were
45
46 calculated from the difference in the urease solution concentration before and after
47
48 immobilization.
49
50
51
52

53 **Labeling of Urease:** Urease was dissolved in PBS buffer (pH 7) in a reaction vial to obtain a 20
54
55 μM solution into which the chemical coupling agents, EDC.HCl (0.4 M) and NHS (0.1 M) were
56
57
58
59
60

1
2
3
4 added and kept for one hour at 4 °C to activate the carboxylic group in urease. Subsequently,
5
6
7 1mg of Rhodamin 123 was added and stirred for 12 hours at room temperature. Figure SI 5
8
9 shows the UV-vis spectrum of urease labeled with Rhodamin 123 (urease-rhodamin) with those of
10
11 urease and Rhodamin 123. The successful labeling of urease was indicated by the same strong
12
13 absorbance at 500 nm of the urease-rhodamin solution with that of the pure Rhodamin 123 solution
14
15 and the blue shift of the urease peak from 276 to 263 nm by amide bond formation²⁹ between
16
17 Rhodamin 123 and urease (marked with arrows). Urease-rhodamin was then immobilized on PAA
18
19 using the same immobilization procedure with urease. After immobilization, the TEM grid cell
20
21 was washed by injecting distilled water into the flow cell to remove the un-reacted urease-rhodamin.
22
23
24
25
26 The urease-rhodamin immobilized on the TEM grid cell was confirmed by fluorescent microscopy
27
28 (Nikon Eclipse, E600POL, Japan).

29
30
31 **Measurements:** Images and videos of the TEM grid cells during (and after) urea injection were
32
33 observed by polarized optical microscopy (POM, Leitz, ANA-006, Germany) with crossed
34
35 polarizers using a CCD camera (Samwon, STC-TC83USB, Korea). ¹H nuclear magnetic
36
37 resonance (NMR, Bruker 400 MHz, Germany) analysis of the PAA-b-LCP was carried out at
38
39 400 MHz. The grey scale intensities of the frames were measured using Adobe Photoshop CS5
40
41 software. The measurements were taken in triplicate and their standard deviations (sds) were
42
43 calculated.

44
45
46
47
48 **Results and Discussion:** The amount of immobilized urease was measured from the optical
49
50 densities obtained by UV-vis spectroscopy. The immobilization density molecules/nm² of the
51
52 urease (N_{urease}) was calculated using equation 1,
53
54

$$N_{urease} = \frac{C_{imb} \times Na}{A \times M_{urease}} \text{----- (1)}$$

1
2
3
4 where C_{imb} , N_{a} , A and M_{urease} are the amounts of immobilized urease in grams, Avogadro's
5 number (6.02×10^{23}), area of the TEM grid in nm^2 ($7.31 \times 10^{12} \text{ nm}^2$), and molecular weight of
6 urease ($4.9 \times 10^5 \text{ g/mole}$), respectively. Figure 1 shows N_{urease} as a function of the urease
7 concentration (C_{urease}). N_{urease} increased with increasing C_{urease} until $C_{\text{urease}} = 20 \text{ }\mu\text{M}$, and then
8 became saturated at $0.17 \text{ molecules/nm}^2$. Therefore, the urease-immobilized TEM grid
9 ($\text{TEM}_{\text{urease}}$) cells prepared with a $20 \text{ }\mu\text{M}$ urease solution were used for further experiments. The
10 immobilization densities of the selected proteins to the PAA brushes were correlated with their
11 molecular masses and sizes. The immobilization densities of horseradish peroxidase (HRP,
12 $4.4 \times 10^4 \text{ g/mol}$), bovine serum albumin (BSA, $6.64 \times 10^4 \text{ g/mol}$) and bovine plasma fibronectin
13 (BPF, $4.99 \times 10^5 \text{ g/mol}$) were 3, 0.6 and $0.1 \text{ molecules/nm}^2$ respectively.²⁸ Binding density of
14 proteins on the PAA brush decreased with increasing their molecular weight. The molecular
15 weight of urease ($4.40 \times 10^5 \text{ g/mol}$) was between those of BPF and BSA, and the immobilization
16 density ($0.17 \text{ molecules/nm}^2$) of urease was also between them despite some discrepancy due to
17 the different experimental set-up, suggesting that the data is in good agreement with the reported
18 values.
19
20
21
22
23
24
25
26
27
28
29
30
31
32
33
34
35
36
37
38
39

40 To confirm the immobilization, urease-*rhodamin* was immobilized on the PAA chains, and
41 observed by fluorescence microscopy. A fluorescent image of the TEM grid cell with the
42 immobilized urease-*rhodamin* (Figure 2a) on the PAA chains showed a green color in the region of
43 the TEM grid, whereas that without the PAA-b-LCP coating (Figure 2b) showed a black image
44 suggesting the successful covalent immobilization of urease on the TEM grid cell.
45
46
47
48
49
50
51

52 **Urea detection:** Figure 3a shows a POM image of $\text{TEM}_{\text{urease}}$ in water at $\text{pH}=7$ under crossed
53 polarizers. A bright image was observed indicating that the $\text{TEM}_{\text{urease}}$ in water at $\text{pH}=7$ has a
54 planar orientation. The aqueous medium in the cell was then replaced with a 20 mM urea
55
56
57
58
59
60

1
2
3
4 solution. The initial planar orientation in the aqueous solution changed to a homeotropic
5 orientation (Figure 3b) in a urea solution. To confirm that the planar to homeotropic (P-H)
6 orientation (Figure 3b) in a urea solution. To confirm that the planar to homeotropic (P-H)
7 change was attributed to the enzymatic reaction of urease, a 20 mM urea solution was injected
8 into the flow cell without immobilizing urease under otherwise similar conditions. A P-H change
9 was not observed (Figure 3d), suggesting that this P-H change was attributed to the hydrolysis of
10 urea by urease. This P-H change might be due to the OH^- ions released by the enzymatic
11 hydrolysis of urea, which increased the pH in the cell and caused the deprotonation and swelling
12 of the PAA chains. The pH-dependent swelling of PAA at the interface could alter the
13 orientational change in the strongly-anchored 5CB in the TEM grid cell. Lee et al. coated 5CB
14 with PAA-b-LCP at the water/LC interface in the TEM grid, and found that the swelling of the
15 PAA chain at high pH caused the homeotropic orientation of the 5CB.²¹ Kinsinger et al.
16 assembled an amphiphilic block copolymer poly(ethylene imine)-b-N-[3-(dimethylamino)-
17 propyl]acrylamide) at the aqueous/LC interface.²⁶ They reported a reversible change in the
18 optical appearance of 5CB upon the alternate exposure to pH 5 and 9 solutions, which they
19 attributed to a conformational change in the hydrophilic chains (shrinkage or swelling) with pH.
20 To determine if a pH change can alter the orientation of 5CB, a basic medium was introduced
21 intentionally by replacing water with a PBS buffer solution (pH=10). Figure 3c shows a POM
22 image of the $\text{TEM}_{\text{urease}}$ with a PBS buffer at pH=10. A similar P-H change was observed,
23 confirming that the P-H change by the addition of urea to the $\text{TEM}_{\text{urease}}$ grid cell was due to an
24 increase in the pH by an enzymatic reaction. Bi et al. used PBA-doped 5CB confined to a
25 penicillinase-immobilized TEM grid to fabricate a pH-sensitive sensor and observed a P-H
26 change by increasing the pH from 6.9 to 7.²⁷ Kim et al. used PAA-b-LCP-coated microdroplets
27 onto which glucose oxidase was immobilized covalently.³⁰ They detected glucose by the radial
28
29
30
31
32
33
34
35
36
37
38
39
40
41
42
43
44
45
46
47
48
49
50
51
52
53
54
55
56
57
58
59
60

1
2
3
4 (homeotropic) to bipolar (planar) change caused by shrinkage of the PAA chains due to the H^+
5 released from the enzymatic oxidation of glucose.
6
7

8
9
10 **Sensitivity:** Figure 4 shows POM images of the TEM grid cells in urea solutions at different
11 concentrations (C_0 s). The initial planar orientation did not change at $C_0 \leq 2$ mM (Figure 4a). At
12 $C_0 = 3$ mM, slight darkness was observed in the TEM grid cell, as shown in Figure 4b.
13
14 Increasing the C_0 to 5 mM resulted in a complete P-H change (Figure 4c). The homeotropic
15 orientation became more evident as C_0 was increased (Figures 4e-f). Under these experimental
16 conditions, the TEM grid urea sensor detected urea at concentrations ≥ 5 mM. Cho et al.
17 fabricated an electrode by cross-linking urease to a polyaniline-Nafion composite and reported a
18 detection limit of 0.03 mM.⁴ Bozgeyik et al. reported a detection limit of 0.1 mM from an
19 amperometric biosensor consisting a urease-immobilized poly(N-glycidylpyrrole-co-pyrrole)
20 thin film.³ Wu et al. immobilized urease on a pH-sensitive carboxylic-poly(vinylchloride) (PVC-
21 COOH) membrane and found a lower detection limit of 0.028 mM.¹² The detection limit of 5
22 mM in this study appears to be higher than the reported ones. On the other hand, the normal urea
23 level in human blood ranged from 2.5 to 6.0 mM and the level from a uraemia patient is ≥ 7
24 mM³¹ so that the detection limit of the TEM_{urease} grid cell is not problematic for checking the
25 chronic level of blood urea. Therefore, the TEM_{urease} grid cell might be useful for pre-scanning
26 the chronic level of urea in blood by the naked eye through a polarized optical microscope under
27 crossed polarizers.
28
29
30
31
32
33
34
35
36
37
38
39
40
41
42
43
44
45
46
47
48

49
50
51 **Blood sample analysis:** Real blood sample was tested to detect urea. A blood sample was
52 collected from a healthy donor and stored in a vial (Note: To avoid microbial activity, the vials
53 were first treated with UV for 15 minutes and the blood was used within one hour after
54
55
56
57
58
59
60

1
2
3
4 collection). Figure 5a shows the response of the TEM_{urease} grid cell to the blood sample. No P-H
5
6 change was observed because the detection limit of the TEM_{urease} grid cell (5 mM) was above the
7
8 normal blood urea level (0.25-0.6 mM). To increase the urea level in the blood, urea was added
9
10 to the normal blood. A P-H change was observed when urea was mixed with the blood to reach a
11
12 urea blood level of approximately 5 mM, as shown in Figure 5b, suggesting that the blood from a
13
14 patient with a urea level in the blood of ≥ 5 mM can be monitored using the TEM_{urease} grid cell.
15
16
17
18

19
20 Blood contains hemoglobin and ascorbic acid (AA). AA is a common electro-active
21
22 species that normally causes interference in electrochemical urea sensors and might also affect
23
24 the P-H change. To confirm the effect of hemoglobin and AA on the P-H change, a mixture
25
26 solution of the hemoglobin (40 mM), ascorbic acid (0.2 mM) and urea (5 and 3 mM) was tested.
27
28 These particular concentrations of hemoglobin and AA were tested because they are the
29
30 maximum possible concentrations in the blood.^{32, 33} The initial planar orientation changed to a
31
32 homeotropic orientation by injecting a mixture solution with 5 mM, as shown in Figure 5c,
33
34 which is similar to the response of the pure urea solution while injecting the mixture with 3 mM
35
36 urea concentration did not change to homeotropic orientation (Figure 5d). This suggests that these
37
38 interference species have no significant impact on urea detection. Although the effects of many
39
40 other components in the blood on the P-H change need to be studied, the present data suggests
41
42 that the TEM_{urease} grid cell might be useful for pre-screening the chronic levels of urea from the
43
44 blood.
45
46
47
48

49
50 **Stability and reproducibility:** An important parameter of the enzyme-based sensor is the long-
51
52 term stability. Urease is a stable enzyme that can be stored at 25 °C for a long time (even one
53
54 month at temperatures up to 60 °C).³⁴ Figure 6 shows the mean gray-scale intensity of the
55
56
57
58
59
60

1
2
3
4
5
6
7
8
9
10
11
12
13
14
15
16
17
18
19
20
21
22
23
24
25
26
27
28
29
30
31
32
33
34
35
36
37
38
39
40
41
42
43
44
45
46
47
48
49
50
51
52
53
54
55
56
57
58
59
60

TEM_{urease} grid cell in an aqueous solution at pH 7 as a function of the period of time. Three different TEM_{urease} grid cells were tested and their gray scale intensities were averaged. No significant change was observed in the grayscale intensity over 10 days. After 10 days, the TEM_{urease} grid cells were tested for urea detection (data not shown), and it was found that it could detect urea in the same way as a freshly prepared TEM_{urease} grid cell. This highlights the stability of the TEM_{urease} grid cell. Therefore, the high stability of the TEM_{urease} grid cell could be achieved by the covalent immobilization of urease, and no urease denaturation occurred in the TEM_{urease} grid cell.

Kinetics: To determine the speed of the urea detection with the TEM_{urease} grid cell, the dynamic response of the LCs were compared at different C₀s. Figures 7i to vi show POM images of the TEM_{urease} grid sensor with time (t_{pass}) after injecting a 8 mM urease solution. The planar orientation of the LCs region deteriorated slowly from the periphery to the center with t_{pass}. After t_{pass} ~5 minutes, the entire square area became homeotropic. Figure 7b shows the grey-scale intensity as a function of time at different C₀s of 3, 5, 8, 20 and 80 mM. The planar orientation has a high grey scale due to the bright color of the planar orientation. The grey-scale intensity decreased with time due to the P-H change and the speed of the P-H transition increased with increasing C₀. The grey-scale intensity decreased slightly at C₀=3 mM and did not reach the saturation level. The times for reaching half of the saturated level (t_{half}) were 250, 160, 63 and 24 seconds at C₀ = 5, 8, 20 and 80 mM, respectively. The decrease in t_{half} with increasing C₀ suggests that the immobilized urease of the TEM_{urease} grid cell hydrolyzed urea effectively. These results also highlight the rapid response and large dynamic range of the TEM_{urease} grid sensor compared to other early reported sensors. For example, Zhong et al.³⁵, Vostiar et al.¹³ and Bozgeyik et al.³ reported 1.0-8.0 mM, 0.02-0.8 mM, 0.1-0.7 mM respectively, using a urea-

1
2
3
4 enzyme field effect transistor made by covering one of the grids of the ions field effect transistor,
5
6 electro-polymerized toluidene blue film on a glassy carbon electrode, and a urease-immobilized
7
8 poly(N-glycidylpyrrole-co-pyrrole) thin film, respectively. Therefore, the TEM_{urease} grid sensor
9
10 performs well at high concentrations in a short response time.
11
12

13
14 **Conclusion:** A TEM grid filled with 5CB on an OTS-coated glass was used to develop a pH-
15
16 sensitive urea biosensor by coating with PAA-b-LCP at the LC/water interface and immobilizing
17
18 urease on the PAA chains through covalent bonding. This TEM_{urease} grid sensor could detect urea
19
20 as low as 5 mM in a sample and showed a large dynamic range, short response time and
21
22 excellent stability with easy detection by the naked eye through a polarized optical microscope
23
24 under crossed polarizers. This could be applicable to detection of urea in the blood without
25
26 interference from hemoglobin and AA. These performances suggest a different way of using the
27
28 unique high sensitivity of liquid crystals to external stimuli as biosensors.
29
30
31
32
33

34 **Supporting Information:** ¹H NMR spectrum of PAA-b-LCP, LB isotherm curve of the PAA-b-
35
36 LCP monolayer on water, Schematic diagram and photograph of the sensor cell containing a
37
38 TEM grid cell, Calibration curve of the urease solutions at $\lambda = 276$ nm, UV-VIS spectra of
39
40 urease, Rhodamin and urease_{-rhodamin}.

41 **Acknowledgements:** This study was supported by National Research Foundation of Korea
42
43 (NRF-2011-0020264)
44
45
46
47
48
49
50
51
52
53
54
55
56
57
58
59
60

References:

1. M. Mascini and G. G. Guilbault, *Anal. Chem.*, 1977, 49, 795-798.
2. D. J. Anderson, B. Guo, Y. Xu, L. M. Ng, L. J. Kricka, K. J. Skogerboe, D. S. Hage, L. Schoeff, J. Wang, L. J. Sokoll, D. W. Chan, K. M. Ward and K. A. Davis, *Anal. Chem.*, 1997, 69, 165-230.
3. İ. Bozgeyik, M. Şenel, E. Çevik and M. F. Abasıyanık, *Curr App Phys.*, 2011, 11, 1083-1088.
4. W.-J. Cho and H.-J. Huang, *Anal. Chem.*, 1998, 70, 3946-3951.
5. G. G. Guilbault and G. Nagy, *Anal. Chem.*, 1973, 45, 417-419.
6. Q.-Z. Hu and C.-H. Jang, *Colloids Surf., B.*, 2011, 88, 622-626.
7. J. Janata, M. Josowicz, P. Vanýsek and D. M. DeVaney, *Anal. Chem.*, 1998, 70, 179-208.
8. W.-Y. Lee, S.-R. Kim, T.-H. Kim, K. S. Lee, M.-C. Shin and J.-K. Park, *Anal. Chim. Acta.*, 2000, 404, 195-203.
9. A. Pizzariello, M. Stredanský, S. Stredanská and S. Miertuš, *Talanta*, 2001, 54, 763-772.
10. B. J. Privett, J. H. Shin and M. H. Schoenfisch, *Anal. Chem.*, 2010, 82, 4723-4741.
11. J. Ruzicka, E. H. Hansen, A. K. Ghose and H. A. Mottola, *Anal. Chem.*, 1979, 51, 199-203.
12. Z. Wu, L. Guan, G. Shen and R. Yu, *Analyst*, 2002, 127, 391-395.
13. I. Vostiar, J. Tkac, E. Sturdik and P. Gemeiner, *Bioelectrochemistry*, 2002, 56, 113-115.
14. P. C. A. Jeronimo, A. N. Araujo and M. Conceicao B.S.M. Montenegro, *Talanta*, 2007, 72, 13-27.
15. R. K. Srivastava, S. Srivastava, T. N. Narayanan, B. D. Mahlotra, R. Vajtai, P. M. Ajayan and A. Srivastava, *ACS Nano*, 2011, 6, 168-175.
16. Y. Bai and N. L. Abbott, *J. Am. Chem. Soc.*, 2012, 134, 548-558.
17. V. K. Gupta, J. J. Skaife, T. B. Dubrovsky and N. L. Abbott, *Science*, 1998, 279, 2077-2080.
18. J. M. Seo, W. Khan and S.-Y. Park, *Soft Matter*, 2012, 8, 198-203.
19. J. M. Brake, M. K. Daschner, Y. Y. Luk and N. L. Abbott, *Science*, 2003, 302, 2094-2097.
20. Y.-Y. Luk and N. L. Abbott, *Curr. Opin. Colloid Interface Sci.*, 2002, 7, 267-275.
21. D. Y. Lee, J. M. Seo, W. Khan, J. A. Kornfield, Z. Kurjib and S. Y. Park, *Soft Matter*, 2010, 6, 1964-1970.
22. W. Khan, J. H. Choi, G. M. Kimb and S. Y. Park, *Lab Chip*, 2011, 11, 3493-3498.
23. W. Khan, J.-M. Seo and S. Y. Park, *Soft Matter*, 2011, 7, 780-787.
24. M. I. Kinsinger, M. E. Buck, N. L. Abbot and D. M. Lynn, *Langmuir*, 2010, 26, 10234-10242.
25. D. S. Miller and N. L. Abbott, *Soft Matter*, 2013, 9, 374-382.
26. M. I. Kinsinger, B. Sun, N. L. Abbott and D. M. Lynn, *Adv. Mater.*, 2007, 19, 4208-4212.
27. X. Bi, D. Hartono and K.-L. Yang, *Adv. Func. Mater.*, 2009, 19, 3760-3765.
28. G. C. M. Steffens, L. Nothdurft, G. Buse, H. Thissen, H. H. ocker and D. Klee, *Biomaterials*, 2002, 23, 3523-3531.
29. A. F. Chaffotte, Y. Guillou and M. E. Goldberg, *Biochemistry*, 1992, 31, 9694-9702.
30. J. Kim, M. Khan and S.-Y. Park, *ACS Appl. Mater. Interfaces*, 2013, 5, 13135-13139.
31. T. W. Meyer and T. H. Hostetter, *N. Engl. J. Med.*, 2007, 357, 1316-1325.

- 1
- 2
- 3
- 4
- 5 32. F. Atsma, I. Veldhuizen, W. de Kort, M. van Kraaij, P. Pasker-de Jong and J. Deinum,
- 6 *Hypertension.*, 2012, 60, 936-941.
- 7 33. S. Ohno, Y. Ohno, N. Suzuki, G.-I. Oma and M. Inoue, *Anticancer Res.*, 2009, 29, 809-
- 8 815.
- 9 34. K. M. R. Kallury, W. E. Lee and M. Thompson, *Anal. Chem.*, 1992, 64, 1062-1068.
- 10 35. L. Zhong, J. Han, G. Li, D. Cui, J. Fan and X. Yang, *Chin J Biotechnol*, 1992, 8, 57-65.
- 11
- 12
- 13
- 14
- 15
- 16
- 17
- 18
- 19
- 20
- 21
- 22
- 23
- 24
- 25
- 26
- 27
- 28
- 29
- 30
- 31
- 32
- 33
- 34
- 35
- 36
- 37
- 38
- 39
- 40
- 41
- 42
- 43
- 44
- 45
- 46
- 47
- 48
- 49
- 50
- 51
- 52
- 53
- 54
- 55
- 56
- 57
- 58
- 59
- 60

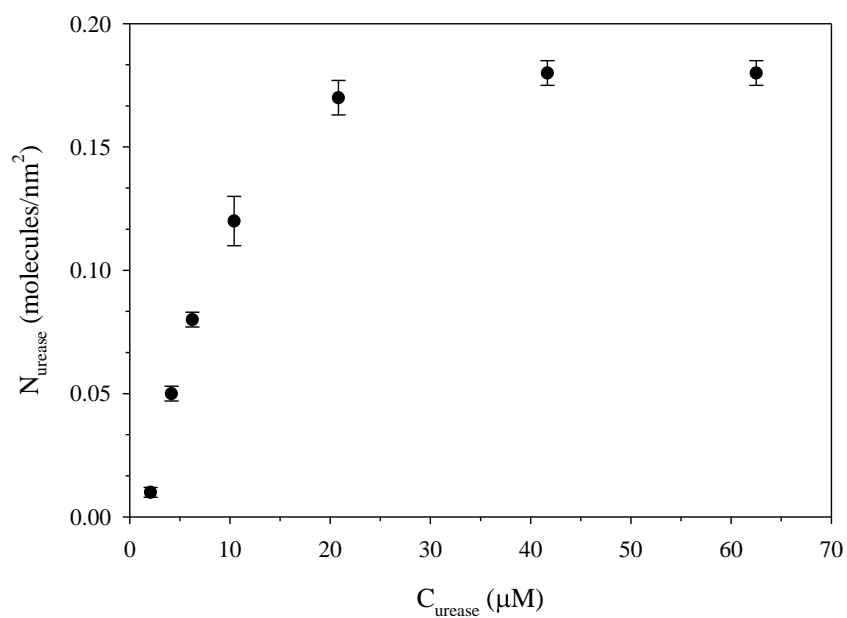


Figure 1. Plot of N_{urease} vs. C_{urease} .

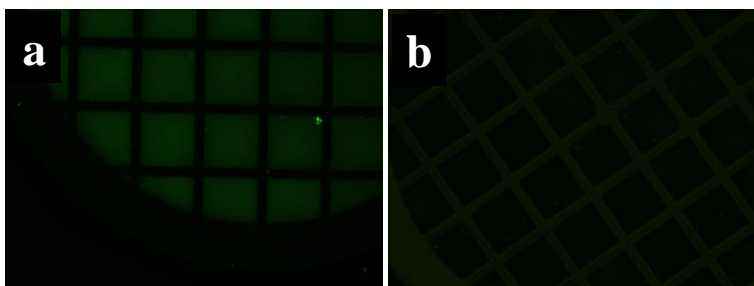


Figure 2. Fluorescent images of the TEM grid cells (a) with and (b) without the immobilization of urease-rhodamin on the PAA chains; the TEM grid cells with and without immobilization were prepared by inserting a 20 μM urease-rhodamine solution into the PAA-b-LCP coated and uncoated TEM grid cells, respectively.

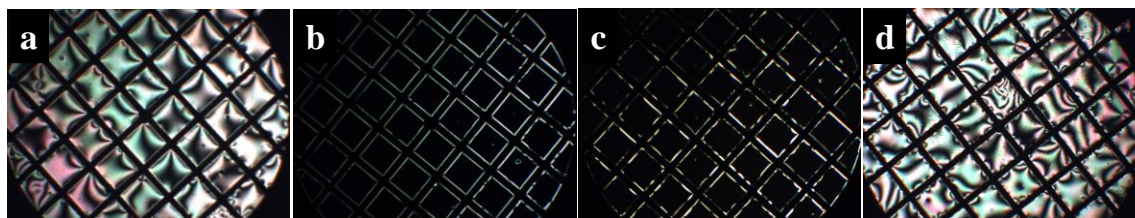


Figure 3. POM images of the TEM_{urease} grid cells under crossed polarizers in (a) water, (b) 20 mM urea solution, and (c) PBS buffer at pH 10; (d) that of the TEM grid without immobilization of urease in a 20 mM urea solution.

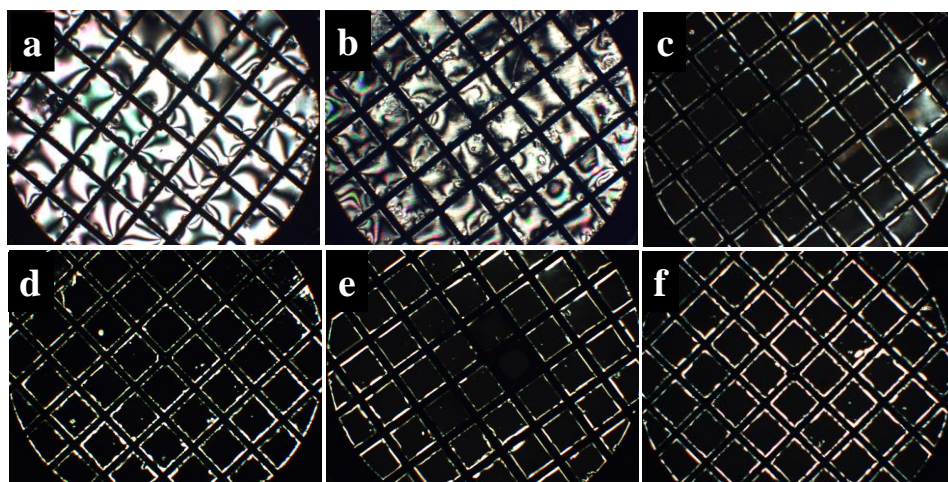


Figure 4. POM images of the TEM grid cells under crossed polarizers with different urea concentrations (C_{0s}) of (a) 2, (b) 3, (c) 5, (d) 8, (e) 20, and (f) 80 mM.

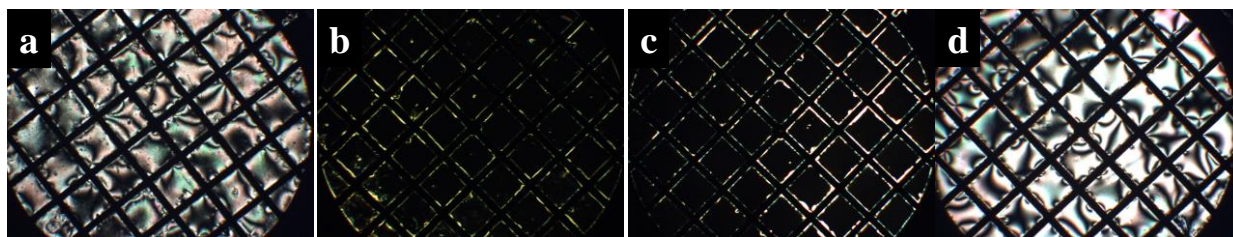


Figure 5. POM images of the TEM grid cells under crossed polarizers after injecting (a) normal pure blood, (b) blood mixed with 5 mM of urea, and (c, d) mixture solutions of hemoglobin (40 mM), ascorbic acid (0.2 mM) and urea ((c) 5 and (d) 3 mM).

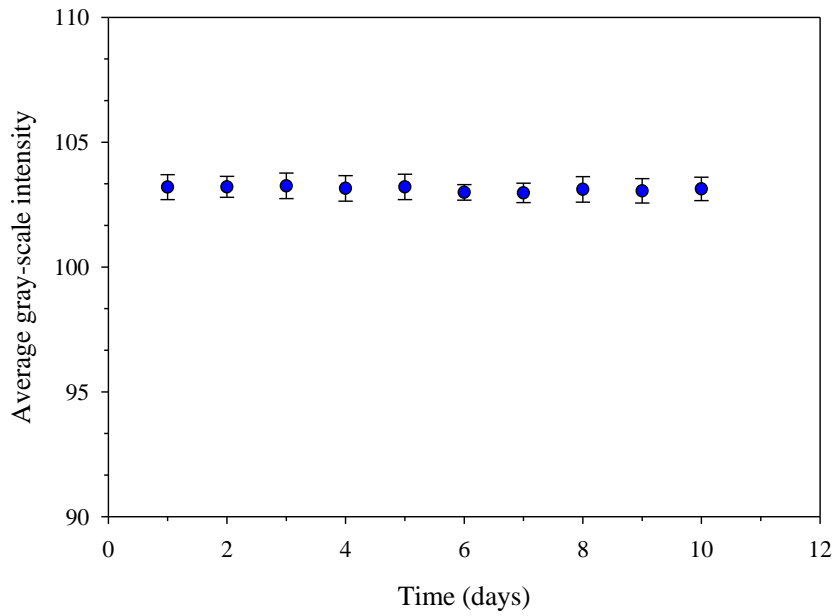
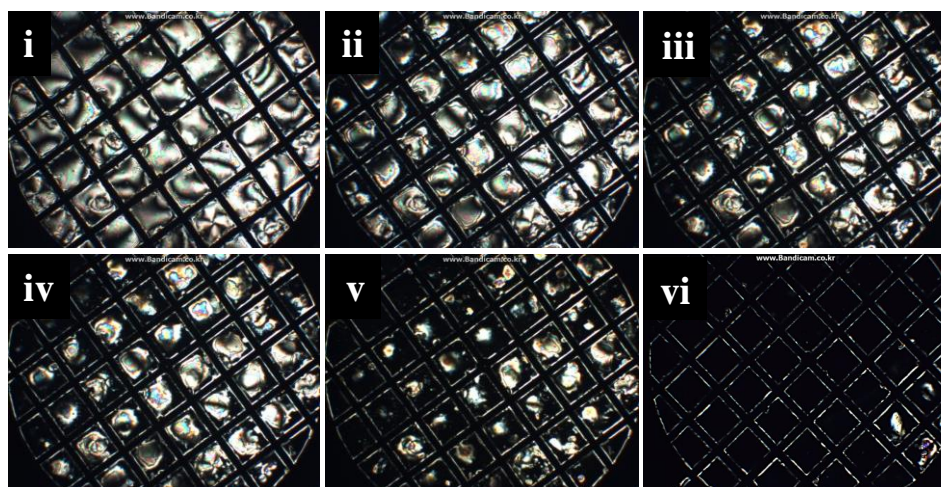
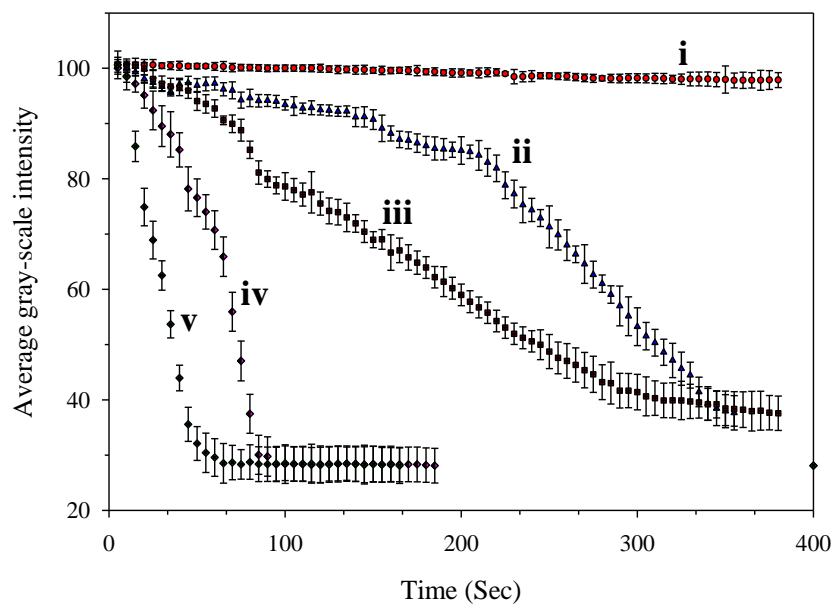


Figure 6. Average gray scale intensity as a function of time.

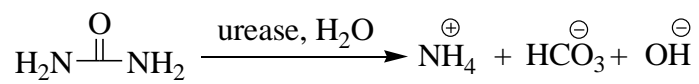


(a)

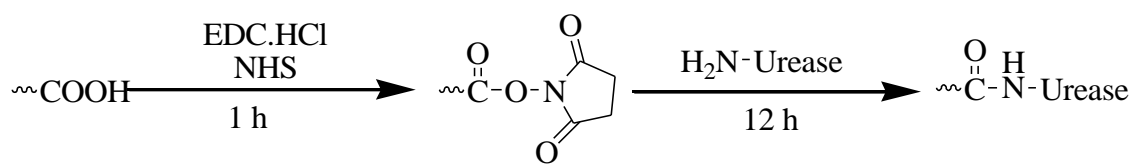


(b)

Figure 7. (a) POM images of the TEM_{urease} grid cells under crossed polarizers with the passage of time (t_{pass}) of (i) 5, (ii) 25, (iii) 50, (iv) 100, (v) 200, and (vi) 450 seconds after injecting a 8 mM urea solution, (b) average gray scale intensity as a function of time at different C_{0s} of (i) 3, (ii) 5, (iii) 8, (iv) 20, and (v) 80 mM.



Scheme 1. Urease-hydrolysis of urea.



11
12
13
14
15
16
17
18
19
20
21
22
23
24
25
26
27
28
29
30
31
32
33
34
35
36
37
38
39
40
41
42
43
44
45
46
47
48
49
50
51
52
53
54
55
56
57
58
59
60

Scheme 2. Chemical immobilization of the urease to PAA chains.